

Article

Tracking Multiple Unmanned Aerial Vehicles through Occlusion in Low-Altitude Airspace

Sufyan Ali Memon ^{1,*}, Hungsun Son ², Wan-Gu Kim ³, Abdul Manan Khan ⁴, Mohsin Shahzad ⁵
and Uzair Khan ⁵¹ Department of Defense Systems Engineering, Sejong University, Seoul 05006, Republic of Korea² Department of Mechanical Engineering, Ulsan National Institute of Science and Technology, Ulsan 44919, Republic of Korea; hson@unist.ac.kr³ Maritime Security and Safety Research Center, Korea Institute of Ocean Science and Technology, Busan 49111, Republic of Korea; kimwangu@kiost.ac.kr⁴ Department of Mechanical and Aerospace Engineering, Bristol University, Bristol BS8 1QU, UK; yf23868@bristol.ac.uk⁵ Department of Electrical and Computer Engineering, COMSATS University Islamabad, Abbottabad Campus, Abbottabad 22060, Pakistan; mohsinshahzad@cuiatd.edu.pk (M.S); uzairkhan@cuiatd.edu.pk (U.K)

* Correspondence: sufyanahmedali@sejong.ac.kr

Abstract: In an intelligent multi-target tracking (MTT) system, the tracking filter cannot track multi-targets significantly through occlusion in a low-altitude airspace. The most challenging issues are the target deformation, target occlusion and targets being concealed by the presence of background clutter. Thus, the true tracks that follow the desired targets are often lost due to the occlusion of uncertain measurements detected by a sensor, such as a motion capture (mocap) sensor. In addition, sensor measurement noise, process noise and clutter measurements degrade the system performance. To avoid track loss, we use the Markov-chain-two (MC2) model that allows the propagation of target existence through the occlusion region. We utilized the MC2 model in linear multi-target tracking based on the integrated probabilistic data association (LMIPDA) and proposed a modified integrated algorithm referred to here as LMIPDA-MC2. We consider a three-dimensional surveillance for tracking occluded targets, such as unmanned aerial vehicles (UAVs) and other autonomous vehicles at low altitude in clutters. We compared the results of the proposed method with existing Markov-chain model based algorithms using Monte Carlo simulations and practical experiments. We also provide track retention and false-track discrimination (FTD) statistics to explain the significance of the LMIPDA-MC2 algorithm.

Keywords: detection; data association; false-track discrimination (FTD); multi-target tracking (MTT); Markov chain model 2 (MC2); probability of target existence (PTE); autonomous vehicle; UAV



Citation: Memon, S.A.; Son, H.; Kim, W.-G.; Khan, A.M.; Shahzad, M.; Khan, U. Tracking Multiple Unmanned Aerial Vehicles through Occlusion in Low-Altitude Airspace. *Drones* **2023**, *7*, 241. <https://doi.org/10.3390/drones7040241>

Academic Editors: Kaiyu Qin, Haitao Nie, Yikang Yang, Xue Li, Jinliang Shao, Lei Shi and Mengji Shi

Received: 2 February 2023

Revised: 24 March 2023

Accepted: 25 March 2023

Published: 30 March 2023



Copyright: © 2023 by the authors. Licensee MDPI, Basel, Switzerland. This article is an open access article distributed under the terms and conditions of the Creative Commons Attribution (CC BY) license (<https://creativecommons.org/licenses/by/4.0/>).

1. Introduction

Multi-target tracking (MTT) is one of the most important problems due to the coalescence nature of the measurements received by a moving-target sensor, such as radar. These uncertain measurements with the coalescence problem result in inaccurate target-state estimates [1]. The MTT system has been widely used in vehicle tracking [2], intelligent transportation systems [3], missile manufacturing [4] and video surveillance [5]. Target identification and behavior analysis becomes more difficult due to occlusion and background-clutter interference in tracking scenes as well as uncertain target motion [6].

Motion capture (mocap) systems have been used in state-of-art technology that utilizes infrared cameras to record the motion of targets in the real-time scenes [7]. The target, such as an unmanned aerial vehicle (UAV), reflects the infrared signals emitted by mocap, which measures the position of the UAV. However, mocap often fails to detect a UAV in the occluded region.

In addition, the MTT system does not know any sort of a priori information regarding unknown objects. Thus, it is always difficult to identify and detect the desired UAV target in the presence of other nuisance objects, such as target thermal noise, birds, clouds and terrain reflection. These unknown random objects generate clutter measurements. The majority of target-associated measurements are concealed due to measurement occlusion in the cluttered airspace surveillance. Thus, MTT faces severe difficulties in determining the target's trajectory and behavior due to low target-detection probabilities P_D in such an environment.

In the cluttered surveillance region, each sensor measurement is either a target or clutter detection. The tracking filter utilizes all available sensor measurements for track initialization and updates, which results in both the true tracks, which follow the target's trajectories and the false tracks, which follow the clutter measurements. The tracking system begins with the initialization of tentative tracks that are usually false tracks, and then a suitable tracking filter is utilized to update the tracks based on the sensor measurements.

Consequently, the tracking filter determines the probability of target existence (PTE) based on the measurements collected up to and including current scan k to evaluate the track-quality measure, which is an important tracking parameter to discriminate between true and false tracks. This technical approach is known as false-track discrimination (FTD) [8]. The FTD attempts to confirm the true tracks using the updated PTE based on the current scan measurements and ultimately terminates the false tracks. The tracking filter system uses the data association algorithms, such as [9–18], to associate the correct measurements to tracks based on the data (measurement) association probabilities. The algorithms described in [9–12] are used for single target tracking (STT), whereas the [13–18] are designed for MTT algorithms. However, only [11,12,16–18] provide PTE as a track-quality measure for FTD evaluation.

The concept of PTE was first developed using a conventional approach known as integrated probabilistic data association filter (IPDA) in [11]. In addition, IPDA provides an approximated Gaussian a posteriori probability density function (PDF) of the target-state estimate; hence, it is also known as a single-scan data-association method. However, integrated track splitting filter (ITS) [12] and multiple-hypothesis tracker [15] are referred to as multi-scan data-association methods because they produce an exponentially growing number of track components and a posteriori measurement PDFs. As a result, both [12] and [15] are computationally complex methods.

The MTT filters use the joint data-association-based methods, such as joint PDA [13,14], joint IPDA [16,17] and joint ITS [18], where the technical term “joint” implies that the same measurements are assigned to tracks. The joint measurements are grouped in the form of cluster tracks. The joint event has no clue about the target measurement. If the measurement is detected from the target, then it may change the feasibility of the detected measurement outcome from other targets or clutter. As a result, these joint data-association methods produce increasing number of feasible joint event hypotheses, which are allocated to tracks globally. These MTT algorithms enumerate all joint measurement to track association hypotheses and compute their measurement probabilities at each scan. Therefore, these joint integrated methods separate the joint measurements in the shape of clusters, compromising severe computational complexity due to the increasing number of clusters. In [16–19], the authors utilized cluster-control techniques in order to limit the computational complexities; however, this effects the estimation performance. We also investigated such methods for MTT but their computations exceed the feasible memory of software.

The intractable computational complexities of the joint data-association-based algorithms are overcome by the linear multi-target (LM) tracking approach, such as LM based on IPDA (LMIPDA) [20–23]. LMIPDA updates a current track by assuming the detected measurement being followed by other tracks as a modified clutter. Thus, LMIPDA avoids the interference of other target tracks (or modified clutters), which allows the tracking

system to ignore the complete process of joint data association. As a consequence of this method, its computational complexity is almost similar to that of the STT methods.

In this research work, we integrate Markov chain two (MC2) and LMIPDA to develop a new robust approach (referred as LMIPDA-MC2) for MTT in the occluded environment. The target existence is a random event—if it is detected, then its PTE is maintained and propagated in each scan using the Markov chain one (MC1) or two (MC2) model. The MC1 is used for the non-occlusion case [11], and MC2 is used for tracking occluded targets [24]. The integrated algorithms, such as IPDA, ITS, joint IPDA, joint ITS and LMIPDA, utilize the MC1 model for propagation of the track PTE. The concept of MC2 was motivated in the [11]; however, the authors used its application in [24–26].

The IPDA based on MC2 model was developed in [24,25]. In [26], the authors utilized the MC2 model in the ITS algorithm for tracking through occlusions. In this conventional method, the authors demonstrated that both IPDA and ITS based on MC1 cannot track targets in occluded scans, and all their tracks become lost. However, ITS-MC2 improved the track retention and FTD at the cost of computational complexities. In [27], the authors utilized the MC2 model in ITS filter [12] for image target tracking in occluding scenarios.

To the best of knowledge, the LMIPDA algorithm is not experienced yet for the occluded targets. This motivated us to investigate the LMIPDA integrated with MC2 for MTT in occluded and high cluttered environments. We modified the propagation and estimation formulas for track initialization and updated them based on the PTE using the MC2 model. We utilized the Monte Carlo simulations to compare the proposed LMIPDA-MC2 method with the LMIPDA-MC1 [20–23], IPDA-MC1 [11] and IPDA-MC2 [24,25] algorithms.

Although, ITS-MC2 is also an example of tracking through occlusions [26,27], it belongs to the class of multi-scan data-association methods. Here, we only investigated single-scan data-association-based methods because they are feasibly applicable for tracking systems at low computational complexity. In addition, we applied the position measurement data produced by a mocap camera to the LMIPDA-MC2 and LMIPDA-MC1 methods for tracking multiple unmanned autonomous vehicles at low altitude in the three-dimensional surveillance region.

In the next section, we discuss the tracking problems and Markov-chain and sensor models. The method of LMIPDA-MC2 is developed in Section 3. The practical implementations, including false-track discrimination (FTD) are discussed in Section 4. Finally, we analyze the method using both Monte Carlo simulations and real-time experiments as illustrated in Section 5 followed by our conclusions in Section 6.

2. Problem Discussion

A sensor with infinite resolutions returns measurements detected from various isolated objects, where each measurement is either originated by a true target or a clutter [26]. We assumed the point targets so that each target creates one or zero measurements per each sensor scan. We also assumed a non-homogeneous Poisson spatial process [28] to generate the clutter measurements. Under these assumptions, the target being followed by a track is not known, and its existence is random. Therefore, we consider the Markov-chain models to update the target existence as well as its detectability as discussed in Section 2.1. A sensor collects the measurements from different objects, including the desired targets as discussed in Section 2.2.

2.1. Markov-Chain Model of Target Existence

We denote the target as well as the track by τ . The propagation of the target existence is modeled by Markov-chain-one (MC1) and -two (MC2) as discussed in [11,24,26,27]. The MC1 consists of two state hypotheses: the first is the probability that the target may exist (denoted by $P\{\chi_k^\tau\}$), and the second hypothesis is the probability that the target may not exist (represented by $\bar{\chi}_k^\tau$). Once the target existence occurs, then it remains detectable in each scan. However, the probability of τ^{th} target existence (PTE) $P\{\chi_k^\tau\}$ is detected with a

low probability of target detection, P_D^τ . The conventional IPDA algorithm uses the MC1 propagation equation to propagate the PTE from scan $k - 1$ to scan k , such as:

$$\begin{aligned}
 P\{\chi_k^\tau\} &= \pi_{1,1}^1 P\{\chi_{k-1}^\tau\} + \pi_{2,1}^1 (1 - P\{\chi_{k-1}^\tau\}), \\
 P\{\bar{\chi}_k^\tau\} &= 1 - P\{\chi_k^\tau\} = \pi_{1,2}^1 P\{\chi_{k-1}^\tau\} + \pi_{2,2}^1 (1 - P\{\chi_{k-1}^\tau\}),
 \end{aligned}
 \tag{1}$$

where $\pi_{i,j}^1$ represents the state transition probability. Unlike the MC1 model, the MC2 model has three hypotheses of the target state [24,26,27]. The first state hypotheses is a probability that the target exists and is detectable as represented by $P\{\chi_k^{\tau,d}\}$; the second state is a event probability $P\{\chi_k^{\tau,n}\}$ that the target exists but it is temporarily undetectable due to occlusion, multi-path fading or target-shadowing; and the third state hypotheses is a probability that the target does not exist $P\{\bar{\chi}_k^\tau\}$ (or $P\{1 - \chi_k^\tau\}$) in scan k . The first two state hypotheses are mutually exclusive events and are represented in terms of probabilities conditioned on the measurements collected by sensor in the current scan k . Thus, we have:

$$P\{\chi_k^\tau\} = P\{\chi_k^{\tau,d}\} + P\{\chi_k^{\tau,n}\}
 \tag{2}$$

The event $\chi_k^{\tau,d}$ has the known P_D^τ , whereas the event $\chi_k^{\tau,n}$ has $P_D^\tau = 0$. The MC2 propagates these probabilities by using the following expressions:

$$\begin{aligned}
 P\{\chi_k^{\tau,d}\} &= \pi_{1,1}^2 P\{\chi_{k-1}^{\tau,d}\} + \pi_{2,1}^2 P\{\chi_{k-1}^{\tau,n}\} + \pi_{3,1}^2 (1 - P\{\chi_{k-1}^\tau\}), \\
 P\{\chi_k^{\tau,n}\} &= \pi_{1,2}^2 P\{\chi_{k-1}^{\tau,d}\} + \pi_{2,2}^2 P\{\chi_{k-1}^{\tau,n}\} + \pi_{3,2}^2 (1 - P\{\chi_{k-1}^\tau\}), \\
 \overline{P\{\chi_k^\tau\}} &= 1 - P\{\chi_k^\tau\} = \pi_{1,3}^2 P\{\chi_{k-1}^{\tau,d}\} + \pi_{2,3}^2 P\{\chi_{k-1}^{\tau,n}\} + \pi_{3,3}^2 (1 - P\{\chi_{k-1}^\tau\}),
 \end{aligned}
 \tag{3}$$

where $\pi_{i,j}^2$ denotes the coefficients of the Markov chain, which define the time updates of each state. These coefficients must be normalized so that:

$$\pi_{1,1}^2 + \pi_{1,2}^2 + \pi_{1,3}^2 = \pi_{2,1}^2 + \pi_{2,2}^2 + \pi_{2,3}^2 = \pi_{3,1}^2 + \pi_{3,2}^2 + \pi_{3,3}^2 = 1.
 \tag{4}$$

As consequence of the Markov coefficients, $\pi_{3,1}^2$ and $\pi_{3,2}^2$ treat the target's non-existence event $P\{1 - \chi_k^\tau\}$ as a target-birth in the track-initialization procedure, and therefore it should not be a part of the track update; otherwise, a false track, which constitutes $P\{1 - \chi_k^\tau\}$ becomes a true track. Thus, to avoid this misinterpretation in $P\{1 - \chi_k^\tau\}$, we assumed that $\pi_{3,1}^2 = \pi_{3,2}^2 = 0$ and $\pi_{3,3}^2 = 1$. The remaining Markov coefficients must be initiated with a track-initialization process by using [8]:

$$\pi_{a,a}^2 = P\{\chi_k^\tau | \chi_{k-1}^\tau\} \approx 1 - \frac{\Delta T_{k,k-1}}{T_{avg}}, \quad a = 1, 2, 3
 \tag{5}$$

where $\Delta T_{k,k-1}$ represents the time difference between scans $k - 1$ and k , and T_{avg} represents the average propagation time period of the target existence. Thus, $\pi_{a,a}^2$ updates the target state existence in scan k , provided that it existed in scan $k - 1$.

We assumed a three-dimensional coordinate system to track the target trajectory state \mathbf{x}_k^τ , which consists of a six-dimensional state vector defined by $\mathbf{x}_k^\tau = [x, y, \dot{x}, \dot{y}, \ddot{x}, \ddot{y}]^t$ (where the superscript t indicates a transpose of matrix). The tracking system uses the following state propagation equation to update the target state from scan $k - 1$ to scan k :

$$\mathbf{x}_k^\tau = \mathbf{F}_{k-1} \mathbf{x}_{k-1}^\tau + \mathbf{v}_{k-1},
 \tag{6}$$

where F_{k-1} represents the state propagation matrix, and v_{k-1} is the Gaussian white-noise of the target model with a zero mean and a known covariance Q_{k-1} .

2.2. Sensor Measurement Model

The sensor model collects a random number of uncertain measurements that originate from random objects, including the desired target. The accumulative set of measurements received by a sensor in scan k is denoted by Z_k . The target measurement in the current scan k is obtained using the following position equation:

$$z_k^\tau = H_k x_k^\tau + w_k, \tag{7}$$

where z_k^τ is the three-dimensional position vector, $H_k = [I_{3 \times 3}, \mathbf{0}_{3 \times 3}]$ (where $I_{3 \times 3}$ and $\mathbf{0}_{3 \times 3}$ represent the identity and zeros matrices, respectively) denotes the measurement matrix, and w_k represents the Gaussian random variable of sensor model with zero mean measurement noise and a known covariance R_k .

The Poisson process [28] generates a non-homogeneous distribution of clutter measurements parameterized by its density, which is a function of coordinate measurements in the surveillance space, which is defined by $\rho_{k,i}^\tau \equiv \rho(Z_{k,i})$ (where i denotes the index of measurements).

3. Integration of LMIPDA and MC2 (LMIPDA-MC2)

The proposed algorithm integrates the LMIPDA with MC2 (LMIPDA-MC2) to deal with occlusion situation in a cluttered surveillance environment. Due to the uncertain sensor measurements, the track remains tentative until the track update, which is based on the measurements collected up to (and including) scan k . We applied the two-point measurement difference formula [8], which uses each pair of measurements accompanied by two subsequent scans $\{Z^k\} = \{Z_k, Z_{k-1}\}$ to initialize a track. Each track is described by its initial PTEs $P\{\chi_{k-1}^{\tau,d} | Z_{k-1}\}$ and $P\{\chi_{k-1}^{\tau,n} | Z_{k-1}\}$. The track calculates the updated probability density function (PDF) of the state measurement $\hat{x}_{k-1|k-1}^\tau$ and its measurement error covariance $\hat{P}_{k-1|k-1}^\tau$ by using the following expressions:

$$\begin{aligned} \hat{x}_{k-1|k-1}^\tau &= \begin{bmatrix} z_k^\tau \\ (z_k^\tau - z_{k-1}^\tau) / T \end{bmatrix}, \\ \hat{P}_{k-1|k-1}^\tau &= \begin{bmatrix} R_k & R_k / T \\ R_k^\tau / T & (R_k + R_{k-1}) / T^2 \end{bmatrix}, \end{aligned} \tag{8}$$

where the hat accent indicates an estimate, and T denotes the sampling time. The predefined initial PTEs $P\{\chi_{k-1}^{\tau,d} | Z_{k-1}\}$ and $P\{\chi_{k-1}^{\tau,n} | Z_{k-1}\}$ are conditioned on the initial measurement set Z_{k-1} and on scan $k - 1$. These initial PTEs are propagated to the next scan k based on the MC2 model by using Equation (3). Thus, Equation (3) becomes:

$$\begin{aligned} P\{\chi_k^{\tau,d} | Z_{k-1}\} &= \pi_{1,1}^2 P\{\chi_{k-1}^{\tau,d} | Z_{k-1}\} + \pi_{2,1}^2 P\{\chi_{k-1}^{\tau,n} | Z_{k-1}\} + \pi_{3,1}^2 (1 - P\{\chi_{k-1}^\tau | Z_{k-1}\}), \\ P\{\chi_k^{\tau,n} | Z_{k-1}\} &= \pi_{1,2}^2 P\{\chi_{k-1}^{\tau,d} | Z_{k-1}\} + \pi_{2,2}^2 P\{\chi_{k-1}^{\tau,n} | Z_{k-1}\} + \pi_{3,2}^2 (1 - P\{\chi_{k-1}^\tau | Z_{k-1}\}). \end{aligned} \tag{9}$$

The track recursion starts from scan $k - 1$ using the updated state PDF and its covariance obtained from Equation (8) as well as the predicted PTEs obtained from Equation (9). LMIPDA-MC2 utilizes the Kalman filter prediction formula [29] to predict the state estimate accompanied by its covariance in the current scan k , such as:

$$\begin{aligned} \bar{x}_{k|k-1}^\tau &= F_k \hat{x}_{k-1|k-1}^\tau, \\ \bar{P}_{k|k-1}^\tau &= F_k \hat{P}_{k-1|k-1}^\tau F_k^\tau + Q_k, \end{aligned} \tag{10}$$

where a bar accent indicates a prediction. The predicted position measurement $\bar{z}_{k,i}^\tau$ (where i indicates the i th measurement) is selected from a set of measurements \mathbf{Z}_k , which were used to develop the validation gate using the measurement-validation selection criterion [11]:

$$\left(\mathbf{Z}_{k,i} - \mathbf{H}_k \bar{\mathbf{x}}_{k|k-1}^\tau\right)^t (\mathbf{S}_k)^{-1} \left(\mathbf{Z}_{k,i} - \mathbf{H}_k \bar{\mathbf{x}}_{k|k-1}^\tau\right) \leq \alpha, \tag{11}$$

where α is the measurement-selection threshold, and $\mathbf{S}_k = \mathbf{H}_k \bar{\mathbf{P}}_{k|k-1}^\tau \mathbf{H}_k^t + \mathbf{R}_k$ is the covariance of the measurement innovation. The probability that the detected measurement is a target measurement falling in the validation gate is known as the gating probability [8], $P_G^\tau = 1 - e^{-0.5\alpha}$. The measurement validation threshold limit is determined from the gating-probability formula. In this method, the size of the validation gate is selected as $\alpha = 13.5$, which corresponds to $P_G^\tau = 0.99$. Thus, the volume of the validation gate U_k in scan k is determined by a priori PDF of the predicted measurement conditioned on \mathbf{Z}_{k-1} , that is $p(\bar{z}_k^\tau | \mathbf{Z}_{k-1})$ falling in the gate. This is defined by:

$$z_k^\tau = \bigcup_i z_{k,i}^\tau, \quad i \in U_k, \tag{12}$$

with the corresponding measurement likelihood [11] expressed as:

$$l_{k,i}^\tau = \frac{1}{\sqrt{2\pi\mathbf{S}_k}} e^{-0.5(\bar{z}_{k,i}^\tau - \mathbf{H}_k \bar{\mathbf{x}}_{k|k-1}^\tau)^t \mathbf{S}_k^{-1} (\bar{z}_{k,i}^\tau - \mathbf{H}_k \bar{\mathbf{x}}_{k|k-1}^\tau)}. \tag{13}$$

The weighted probability $P_{k,i}^\tau$ that the validated measurement $\bar{z}_{k,i}^\tau$ with respect to track τ is originated by a τ th target measurement z_k^τ is obtained by using the following [20]:

$$P_{k,i}^\tau = P_D^\tau P_G^\tau P\{\chi_k^{\tau,d} | \mathbf{Z}_{k-1}\} \frac{l_{k,i}^\tau / \rho_{k,i}^\tau}{\sum_{i=1}^{m_k} l_{k,i}^\tau / \rho_{k,i}^\tau}, \tag{14}$$

where m_k denotes the number of validated measurements. These a priori probabilities of the predicted measurements are mutually exclusive events so that only one measurement is a target detection in scan k . Note that, if there is no measurement selection $i = 0$ from Equation (11), then $l_{k,i}^\tau = 0$, and thus $P_{k,i}^\tau = 0$. In addition, the a priori probability that the predicted measurement is not followed by neighbored track σ in the coordinate of the τ th track is defined by [20]:

$$\bar{P}_{k,i}^\tau = \prod_{\sigma \in \Delta} (1 - P_{k,i}^\sigma), \tag{15}$$

where Δ denotes the set of tracks excluding τ th track, which is in the update process, and σ belongs to Δ . LMIPDA-MC2 assumes the predicted measurements followed by a track σ as modified clutter (or fake target) measurement because it is actually detected by the τ th track. Consequently, the clutter measurement density $\rho_{k,i}^\tau$ is updated by a modified clutter measurement that is calculated by [20]:

$$\mu_{k,i}^\tau = \rho_{k,i}^\tau + \sum_{\substack{\sigma=1 \\ \sigma \neq \tau}}^{\sigma=\tau_n} \frac{l_{k,i}^\sigma P_{k,i}^\sigma}{(1 - P_{k,i}^\sigma)}, \tag{16}$$

where τ_n indicates the number of tracks, and $\mu_{k,i}^\tau$ denotes the updated clutter measurement density calculated in the coordinate of $\bar{z}_{k,i}^\tau$ with respect to the τ th track.

Equation (16) is used to obtain the track-likelihood ratio and data-association probabilities [24] of the predicted measurements $\bar{z}_{k,i}^\tau$ by using Equations (17) and (18), respectively.

$$\lambda_{k,i}^\tau = 1 - P_D^\tau P_G^\tau + P_D^\tau P_G^\tau \sum_{i=1}^{m_k} \frac{l_{k,i}^\tau}{\mu_{k,i}^\tau}, \tag{17}$$

and

$$\beta_{k,i}^\tau = \frac{P_D^\tau P_G^\tau \frac{l_{k,i}^\tau}{\mu_{k,i}^\tau} P\{\chi_k^{\tau,d} | \mathbf{Z}_{k-1}\}}{\lambda_{k,i}^\tau P\{\chi_k^{\tau,d} | \mathbf{Z}_{k-1}\} + P\{\chi_k^{\tau,n} | \mathbf{Z}_{k-1}\}}. \tag{18}$$

If the predicted measurement being tracked in current scan k is not originated by a target, then the data association probability with respect to $i = 0$ becomes [24]:

$$\beta_{k,0}^\tau = \frac{1 - P_D^\tau P_G^\tau P\{\chi_k^{\tau,d} | \mathbf{Z}_{k-1}\} + P\{\chi_k^{\tau,n} | \mathbf{Z}_{k-1}\}}{\lambda_{k,0}^\tau P\{\chi_k^{\tau,d} | \mathbf{Z}_{k-1}\} + P\{\chi_k^{\tau,n} | \mathbf{Z}_{k-1}\}}, \tag{19}$$

where $\lambda_{k,0}^\tau = 1 - P_D^\tau P_G^\tau$.

LMIPDA-MC2 obtains target-state estimates with respect to the τ th track by using the Kalman-filter-update formula [29] as expressed in the following equations:

$$\begin{aligned} \hat{\mathbf{x}}_{k|i}^\tau &= \bar{\mathbf{x}}_{k|i-1}^\tau + \mathbf{K}_k \left(\bar{\mathbf{z}}_{k,i}^\tau - \mathbf{H}_k \bar{\mathbf{x}}_{k|i-1}^\tau \right), \\ \hat{\mathbf{P}}_{k|i}^\tau &= \bar{\mathbf{P}}_{k|i-1}^\tau - \mathbf{K}_k \mathbf{H}_k \bar{\mathbf{P}}_{k|i-1}^\tau, \end{aligned} \tag{20}$$

where $\mathbf{K}_k = \bar{\mathbf{P}}_{k|i-1}^\tau \mathbf{H}_k^t \mathbf{S}_k^{-1}$ is known as the Kalman gain in scan k . These target-state estimates corresponding to the validated measurements $\bar{\mathbf{z}}_{k,i}^\tau$ are approximated by one Gaussian mean and covariance using the following equations:

$$\hat{\mathbf{x}}_{k|k}^\tau = \sum_{i=1}^{m_k} \beta_{k,i}^\tau \hat{\mathbf{x}}_{k|i}^\tau \tag{21}$$

and

$$\hat{\mathbf{P}}_{k|k}^\tau = \sum_{i=1}^{m_k} \beta_{k,i}^\tau \left(\hat{\mathbf{P}}_{k|i}^\tau + \hat{\mathbf{x}}_{k|i}^\tau \left(\hat{\mathbf{x}}_{k|i}^\tau \right)^t \right) - \hat{\mathbf{x}}_{k|k}^\tau \left(\hat{\mathbf{x}}_{k|k}^\tau \right)^t. \tag{22}$$

Similarly, each updated target-state estimate is retrieved in the next scan $k + 1$ to obtain the predicted state estimate $\bar{\mathbf{x}}_{k+1}^\tau$ and its covariance $\bar{\mathbf{P}}_{k+1}^\tau$ conditioned on the \mathbf{Z}_{k-1} by using the prediction Equation (10).

LMIPDA-MC2 evaluates the track quality based on the total updated PTE using Equation (2), which is the sum of the following two updated probabilistic events conditioned on the measurement set \mathbf{Z}_k in the current scan k :

$$\begin{aligned} P\{\chi_k^{\tau,d} | \mathbf{Z}_k\} &= \frac{\lambda_{k,i}^\tau P\{\chi_k^{\tau,d} | \mathbf{Z}_{k-1}\}}{1 - (1 - \lambda_{k,i}^\tau) P\{\chi_k^{\tau,d} | \mathbf{Z}_{k-1}\}}, \\ P\{\chi_k^{\tau,n} | \mathbf{Z}_k\} &= \frac{P\{\chi_k^{\tau,n} | \mathbf{Z}_{k-1}\}}{1 - (1 - \lambda_{k,i}^\tau) P\{\chi_k^{\tau,d} | \mathbf{Z}_{k-1}\}}, \end{aligned} \tag{23}$$

so that the total updated probability of occluded target existence becomes [24]:

$$P\{\chi_k^\tau | \mathbf{Z}_k\} = P\{\chi_k^{\tau,d} | \mathbf{Z}_k\} + P\{\chi_k^{\tau,n} | \mathbf{Z}_k\} \tag{24}$$

The proposed LMIPDA-MC2 method recursively iterates from Equation (8) to Equation (24) to obtain target-state estimates with respect to the τ th track in each scan k . Equation (24) is used to evaluate the FTD, which is an important parameter in multi-target tracking. This method is illustrated using a flowchart in Figure 1, which also shows the procedure of multi-target state statistics evaluation as depicted in the dotted-lined box. The procedure of the algorithm's statistics calculation is also described in the next section.

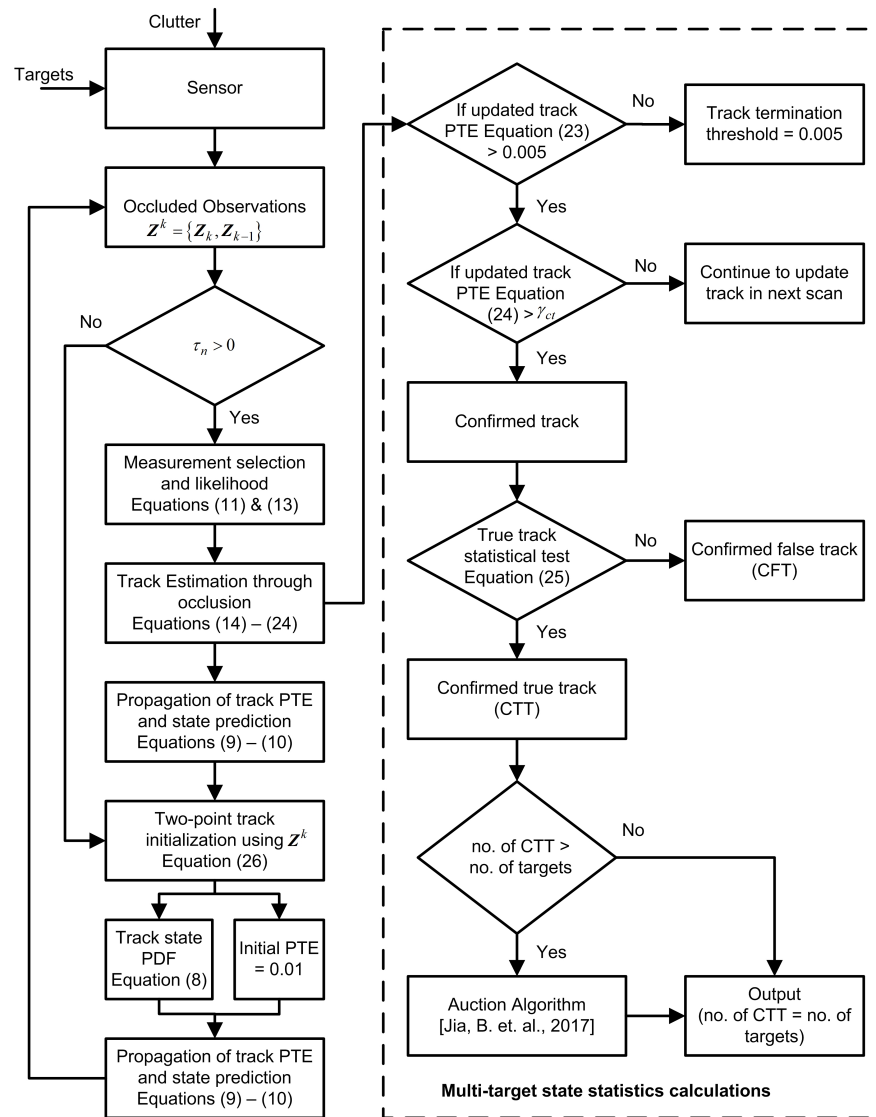


Figure 1. The flowchart of the LMIPDA-MC2 method [30].

4. False-Track Discrimination (FTD)

In general, the track is tentative; therefore, it is necessary to evaluate the nature of a track. We used PTE to determine the track quality, which is required for FTD. We assumed the predefined confirmation and termination thresholds to evaluate the track quality. A track attains the confirmed status if its updated PTE value surpasses the confirmation threshold (as indicated by γ_{ct} in Figure 1). However, a track terminates its status if its updated PTE value becomes lower than the termination threshold. Therefore, the track-PTE is recursively updated and propagated in each scan k using Equations (9) and (24).

A track could be lost and concealed due to the occlusion of an uncertain target and clutter measurements leading it to track unknown measurements in the surveillance airspace. To identify the confirmed track status in the occlusion situation, the LMIPDA-MC2 utilizes the chi-squared statistic evaluation criteria [8,31], which is given by:

$$(\hat{x}_{k|k}^T - x_k^T)^T (P_{1|1}^T)^{-1} (\hat{x}_{k|k}^T - x_k^T) < \eta, \tag{25}$$

where $P_{1|1}^T$ represents the covariance matrix of sensor measurement noise, and η indicates the minimum distance threshold between the estimated track state $\hat{x}_{k|k}^T$ and the desired target state x_k^T . Thus, a track is referred to as a confirmed true track (CTT) if its minimum normalized distance squared (MNDS) value $(\hat{x}_{k|k}^T - x_k^T)$ is within the threshold limit ≤ 20 ;

otherwise, it becomes a confirmed false track (CFT) as depicted in the dotted-line box in Figure 1. This threshold value is a designer's choice that depends on the target model as well as the complexities in the tracking system. We applied Equation (25) using each confirmed track state estimate (obtained in Equation (21)) and each desired target state (expressed by Equation (6)) in each scan k .

In the occlusion situation, it is also difficult to identify the target's identity, even if we have obtained the CTT. Some of the CTTs follow the same target, which tends to mislead the identities of the tracks as well as targets. Therefore, the LMIPD-MC2 exploits the bidding method using the auction algorithm [30] as indicated in Figure 1. The MNDS parameter obtains the weighted benefit score with respect to each CTT, which raises the bid for asynchronous CTTs. Therefore, the benefit score of each CTT is compared so that the winning bid with the highest benefit score is obtained for a asynchronous CTT. As result, the number of CTTs becomes equal to the number of targets in each scan k .

5. Illustrative Simulation and Experimental Results

We analyzed the statistics of the proposed LMIPDA-MC2 method using Monte Carlo simulations and real-time experiments for tracking multi-targets in occlusions at low-altitude airspace. In the following subsections, we compare the analytical results of LMIPDA-MC2 and existing reference methods using both simulations and experiments.

5.1. Monte Carlo Simulation Results

In the simulation scenario, we considered the two-dimensional occluded surveillance environment, which is 450 m wide and 600 m long. The multi-targets are moving at low-altitude airspace through the clutters with a heavy measurement density of $\rho_{k,i} = 1 \times 10^{-4} \text{ m}^{-2}$ as shown in Figure 2. In this occluded surveillance area, a sensor generates the measurements corrupted by white noise with a known covariance $\mathbf{R}_k = 25\mathbf{I}_{2 \times 2}$ (where $\mathbf{I}_{2 \times 2}$ represents the identity matrix). The average number of clutters per each scan is 45. In addition, the target dynamic model produces the process noise, $q = 0.75 \text{ m}^2/\text{s}^4$, which further corrupts the target state, which has a probability of detection of $P_D^T = 0.9$.

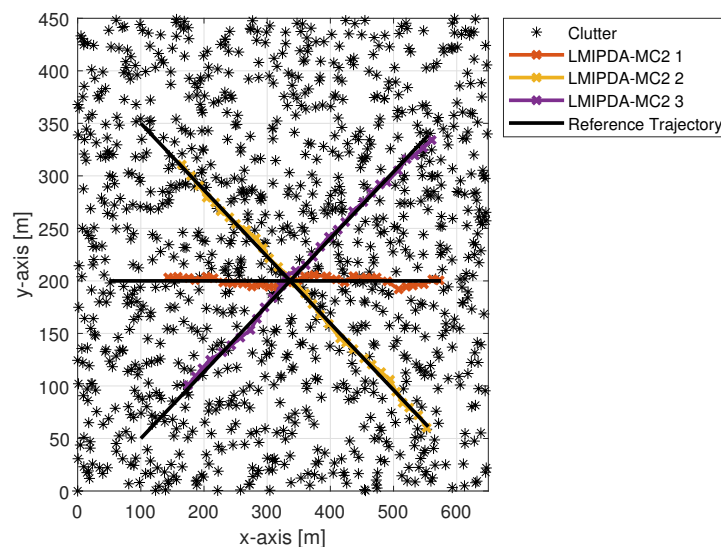


Figure 2. Multi-target tracking in occlusion and clutter.

Under the circumstances described above, we compare the MTT performance of the proposed LMIPDA-MC2 method with the LMIPDA-MC1, IPDA-MC2 and IPDA-MC1 algorithms in terms of the estimation accuracies, track retention and track-quality measure of FTD. These algorithms were simulated for 200 Monte Carlo simulation runs with 36 scans per run. The sampling time in each scan was assumed to be $T = 1 \text{ s}$. Approximately, 63,600

(318 per run) tracks were initialized by each algorithm. These tracks were initialized using the following two-scan velocity formula [8]:

$$V_{k,i} = \frac{\sqrt{(X_{k-1,i} - X_{k,i})^2 + (Y_{k-1,i} - Y_{k,i})^2}}{T} \leq V_{max}, \quad (26)$$

where V_{max} denotes the target's maximum velocity, which equals 25 m/s, $X_{k-1,i}$, $X_{k,i}$, $Y_{k-1,i}$, and $Y_{k,i}$ denotes the i th measurement in the coordinates of two successive scan's measurement sets, $\mathbf{Z}^k = \{\mathbf{Z}_{k-1}, \mathbf{Z}_k\}$. A track is initialized when the resultant i th measurement velocity $V_{k,i}$ satisfies Equation (26).

The two-dimensional initial position vectors of targets 1, 2 and 3 are [50; 200], [100; 350] and [100; 50], respectively, as shown in Figure 2. These closely moving targets in the occlusion certainly crossed near the coordinate points at approximately [335; 200]m in scans 19 and 20; in which, Targets 2 and 3 met in scan $k = 19$ at the same position with only 3 m difference in their altitude. The information about the initial positions of targets is supplied to the LMIPDA-MC2 algorithm but their dynamic motion is not known. The information about the two-dimensional velocity vector of the target state is obtained by using Equation (26) in the track-initialization process. Therefore, the target's identities are untagged, and their measurements are randomly merged with the background clutters. Thus, the proposed filter uses a series of position measurements observed over time using Equation (7), including statistical noise and other measurement inaccuracies to produce estimates of unknown state variables that tend to be more accurate and realistic scenarios.

In the surveillance space, the occlusion occurred in scans $k = 19$ to $k = 23$. In the occlusion situation, Figure 2 also illustrates the effective tracking results of the proposed LMIPDA-MC2 algorithm. We assumed a nearly constant velocity model for target state propagation with the following propagation matrices [8]:

$$F_{k-1} = \begin{bmatrix} \mathbf{I}_{2 \times 2} & T\mathbf{I}_{2 \times 2} \\ \mathbf{0}_{2 \times 2} & \mathbf{I}_{2 \times 2} \end{bmatrix}, \quad (27)$$

$$Q_{k-1} = q \begin{bmatrix} 0.25T^4\mathbf{I}_{2 \times 2} & 0.5T^3\mathbf{I}_{2 \times 2} \\ 0.5T^3\mathbf{I}_{2 \times 2} & T^2\mathbf{I}_{2 \times 2} \end{bmatrix}, \quad (28)$$

where $\mathbf{0}_{2 \times 2}$ is the 2×2 zeros matrix. The proposed LMIPDA-MC2 and the reference method IPDA-MC2 utilize the MC2 model for track maintenance and update the process in each scan k using a three-state target-existence transition matrix [24,25] as expressed in Equation (29). However, the IPDA-MC1 [11] and LMIPDA-MC1 [20,21] algorithms utilize the dynamics of the target existence event using a two state MC1 model with a target transition probability matrix as expressed in Equation (30).

$$\pi = \begin{bmatrix} 0.98 & 0.02 & 0.02 \\ 0.02 & 0.98 & 0.02 \\ 0 & 0 & 1 \end{bmatrix}, \quad (29)$$

$$\pi = \begin{bmatrix} 0.98 & 0.02 \\ 0 & 1 \end{bmatrix} \quad (30)$$

Each track was initialized with a lowest PTE of 0.01, and its track quality PTE was evaluated by varying the track confirmation threshold in response to obtain almost the same number of CFTs (≈ 3). Each confirmed track state was consistently confirmed unless the track's PTE reached the lowest track-termination threshold of 0.005.

The technical parameters discussed above were applied to IPDA-MC1, IPDA-MC2, LMIPDA-MC1 and LMIPDA-MC2 for a fair comparison analysis. Figure 3 shows the results of FTD in terms of number of CTTs with respect to all targets. The targets are moving in occluded scans $k = 19$ to $k = 23$ as shown in Figure 2. In these occluded scans, the track

retention of IPDA-MC1 and IPDA-MC2 is quite weak because of undetectable targets, so that both methods lose almost 70% of the number of CTTs in scan $k = 20$ as depicted in Figure 3. We can see that standard LMIPDA has a slower response to FTD because it uses the MC1 model for track PTE propagation in occlusion. The LMIPDA-MC1 method also reduces track retention in these occluded scans and then, from scan $k = 23$, it improves the track PTE for FTD as depicted in Figure 3. Therefore, there is a high chance of track loss if we use the MC1 model for PTE propagation in the occlusion. The FTD results of LMIPDA-MC1 and LMIPDA-MC2 have similar trends of track confirmation near the end scans. However, LMIPDA-MC2 quickly and accurately builds up the track-quality measure of PTE. Thus, the number of CTTs in LMIPDA-MC2 is the highest in each scan k as shown in Figure 3.

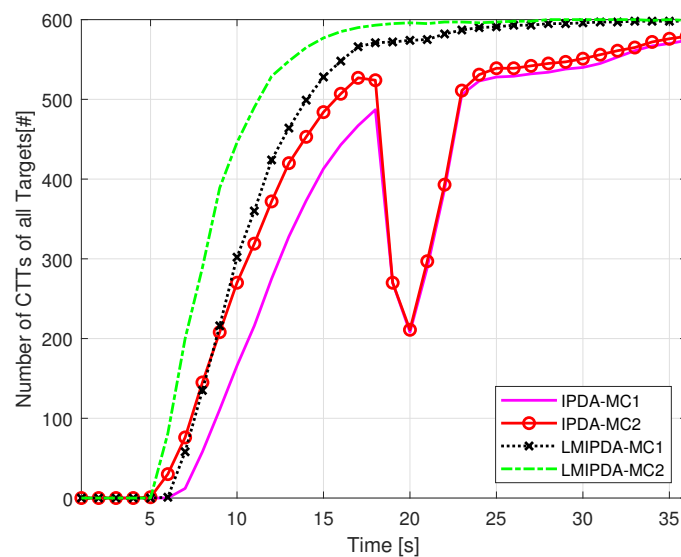


Figure 3. Number of confirmed true tracks (CTTs) out of 200 runs.

We verified the FTD results again using Monte Carlo simulation for 1000 runs as shown in Figure 4. The simulation parameters and surveillance scenario is the same as before. We can see that the reference methods have slower rates of track confirmation. Both the IPDA-MC1 and IPDA-MC2 algorithms lost almost 50% CTT. This track lost is due to the measurement occlusion. The standard LMIPDA method, which uses the MC1 model lost few of its confirmed tracks near the occluded scans $k = 19$ to $k = 23$. However, after occlusion scan $k = 22$, the tracking response of LMIPDA improved well as compared to IPDA-type filters. In comparison to the reference methods, the proposed LMIPDA-MC2 significantly improved the FTD performance. Thus, the purpose of the LMIPDA-MC2 is useful and feasible in the application of multi-target-tracking systems.

The position-estimation error of the targets ($\tau = 1, 2, 3$) is calculated using the root mean square error (RMSE) process with respect to each CTT as illustrated in Figure 5a–c. The RMSE statistics were accumulated for only 200 simulation runs since the analytical results remained the same. Both LMIPDA-MC1 and LMIPDA-MC2 had similar trends of RMSE statistics; however, the RMSEs of both IPDA-MC1 and IPDA-MC2 were higher specifically at the occluded scans $k = 20$ to $k = 22$ as depicted in Figure 5. This shows that the growth of track PTE is slow in case of both IPDA-MC1 and IPDA-MC2 in the occluded and cluttered environment. The RMSE statistics of the algorithms converged at the final scan because they used the same measurement set collected in scan $k = 36$ to conclude the simulations.

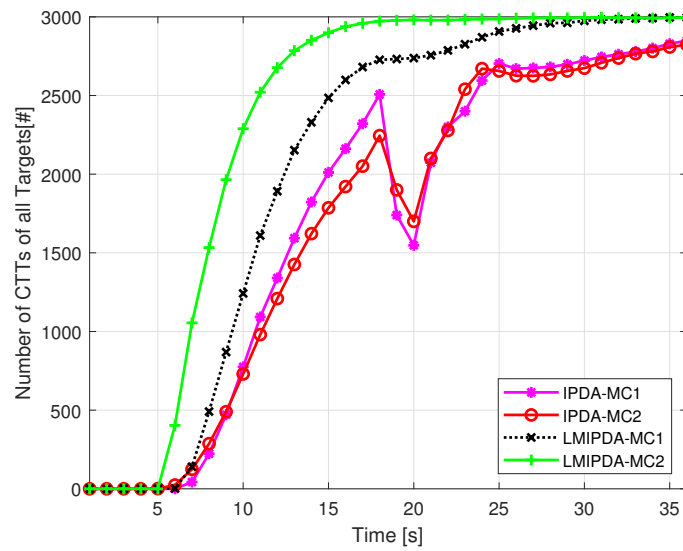
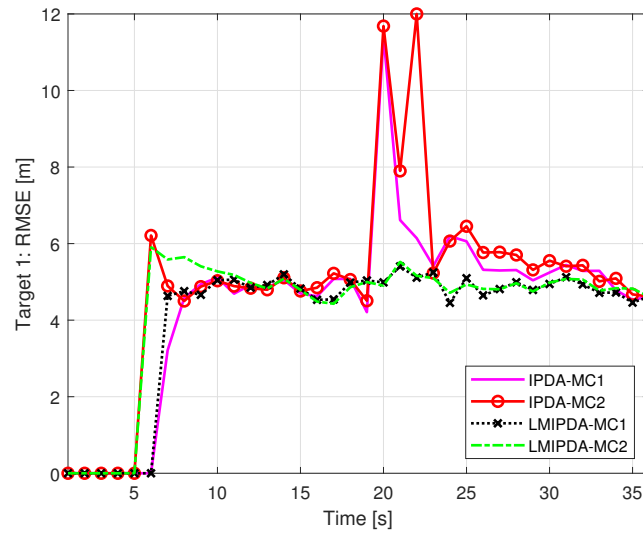
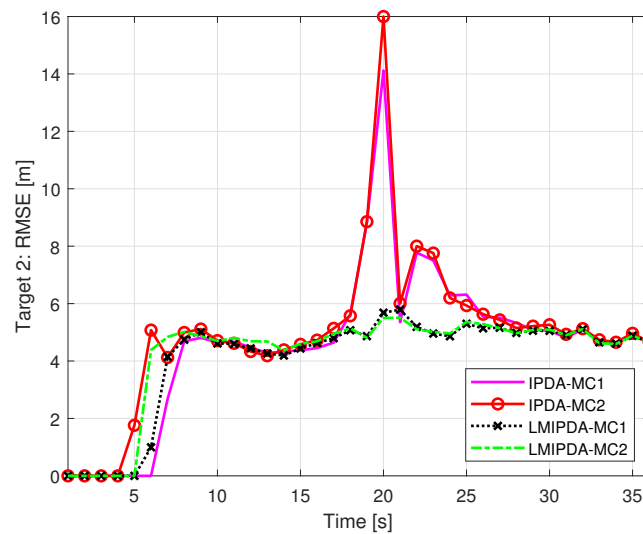


Figure 4. Number of confirmed true tracks (CTTs) out of 1000 runs.



(a)



(b)

Figure 5. Cont.

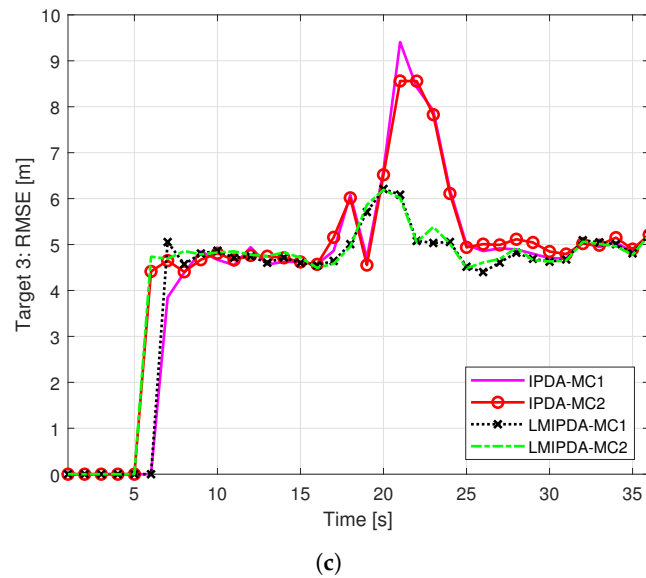


Figure 5. Root mean square errors (RMSEs). (a) RMSE of Target 1. (b) RMSE of Target 2. (c) RMSE of Target 3.

We evaluated the CTT retention statistics of the algorithms accounting 200 runs of simulations as detailed in Table 1. A unique identity index was assigned to each initialized track. We checked the identity of CTT before and after the intersection coordinate point of the multi-targets in order to find the following analytical results:

- Case: to obtain the total number of confirmed track pursuing the original τ th target in scan $k = 13$.
- Okay: to obtain the total number of CTTs that still retain the original τ th target in scan $k = 28$.
- Switched: to obtain the total number of CTTs that switched the original target to some other CTT and now pursue a different target in scan $k = 28$.
- Lost: to obtain the total number of CTTs that were lost in scan $k = 28$ because they were either terminated or they became CFTs.
- End: to obtain the total number of CTTs at the end scan $k = 36$.
- Execution time [s]: the average execution time per run.

Table 1. Target-track-retention statistics of the algorithms.

Algorithm	Case	Okay	Switched	Lost	End	time [s]
IPDA-MC1	517	449	38	30	574	0.3
IPDA-MC2	513	422	56	35	561	0.4
LMIPDA-MC1	568	550	16	2	595	0.2
LMIPDA-MC2	600	598	2	0	599	0.5

As listed in Table 1, the LMIPDA-MC2 algorithm had the highest number of Case, Okay and End and additionally, the lowest number of Switched and Lost when compared to the other methods. In fact, the proposed method had 0 lost out of 200 runs. Table 1 also details the average execution time per run of the algorithms. We utilized the MATLAB R2020b software on the 11th Intel Core™ i7-1165G7 (@ 2.80 GHz, 2.80 GHz) computer for programming the algorithms.

5.2. Experimental Results

In the experimental scenario, we compared the statistical results of the proposed LMIPDA-MC2 algorithm and the conventional LMIPDA-MC1 method in the three-dimensional occluded surveillance airspace. The set of position measurements used in this paper was

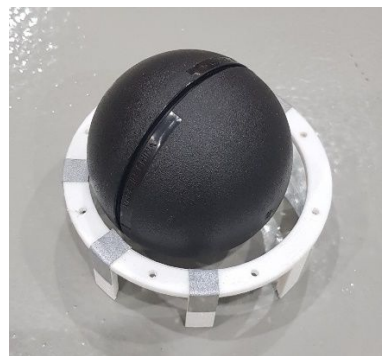
originally published in [32] by the corresponding author of this paper. In the experiment, we utilized the original position data to evaluate the proposed LMIPDA-MC2 method. In [32], the surveillance area was assumed to be 3 m long along the x-axis and 4 m wide along the y-axis as shown in Figure 6a. This region rendered three autonomous vehicles (battery-operated vehicles) and a multi-rotor unmanned aerial vehicle (UAV) as shown in Figure 6b and 6c, respectively. This type of MTT system consisted of the motion capture (mocap) camera, UAV model, autonomous vehicle and a computer, which was used for analyzing the statistical results of the tracking method as shown in Figure 6d.



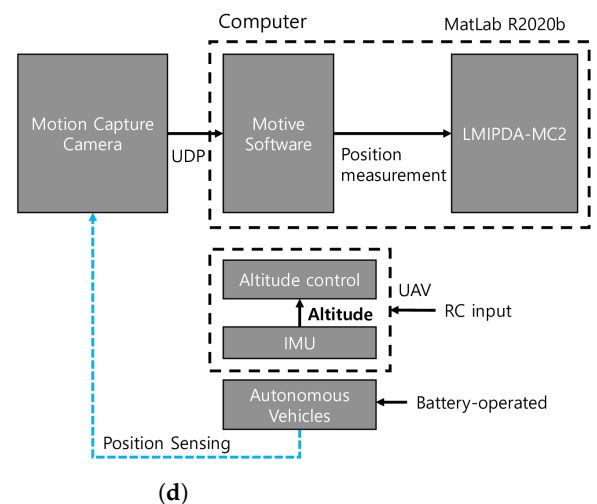
(a)



(b)



(c)



(d)

Figure 6. Experimental platform: (a–c) are reprinted from Expert Systems with Applications, 177, Myunggun Kim, Sufyan Ali Memon, et al., Dynamic based trajectory estimation and tracking in an uncertain environment, Page No. 7, Copyright (2021), with permission from Elsevier. (a) Surveillance region. (b) UAV. (c) Autonomous vehicle. (d) Experimental setup.

We utilized four OptiTrack Prime 13 mocap cameras in a three-dimensional surveillance environment. The Motive 2.2 (a mocap software, which was installed in a computer) was used to measure the position measurement of each target, which was simultaneously

returned to the tracking algorithm in each scan. The communication between the mocap camera and Motive was linked by a User Datagram Protocol (UDP) as depicted in Figure 6d. The UAV is controlled by a RC (remote control) input, while autonomous vehicles can move freely without user control. A UAV started from an initial position $[-1.98, -1.34, -0.15]^t$, and the other vehicles moved randomly in the three-dimensional surveillance area. Therefore, the motion and the trajectory behavior of each target were not known to the algorithm. The typical values of the experimental parameters are shown in Table 2.

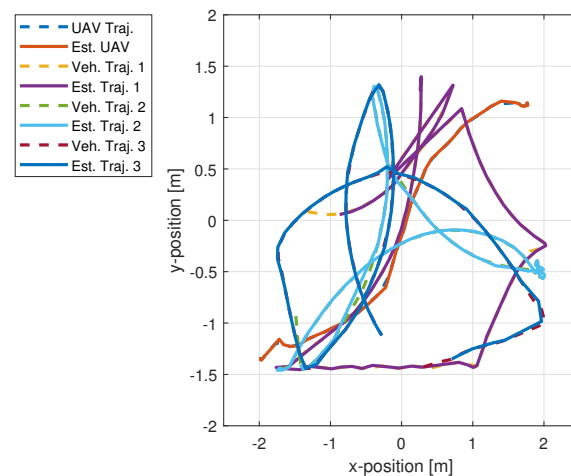
Table 2. Experimental parameters.

Parameter	Description	Value
A	Surveillance region	$[3, 4, 4]^t$ m
R_k	Measurement noise covariance	$0.08I_{3 \times 3}$
Number of scans	Number of time steps	83
T	Sampling time between scans	0.25 s
P_D	Detection probability	0.8
$\rho_{k,i}^r$	Clutter measurement density	$5 \times 10^{-4} \text{ m}^{-3}$
α	Validation measurement-selection threshold	5

The proposed LMIPDA-MC2 was applied to the tracking system, which received the measurements from the mocap system and estimated their measurements simultaneously for tracking multi-targets in each scan. The target's identities were untagged, and their position measurements were returned by mocap markers, which were placed on each target. We can see the mocap markers (silver colored) stucked in both autonomous vehicles and a UAV as shown in Figure 6b and 6c, respectively.

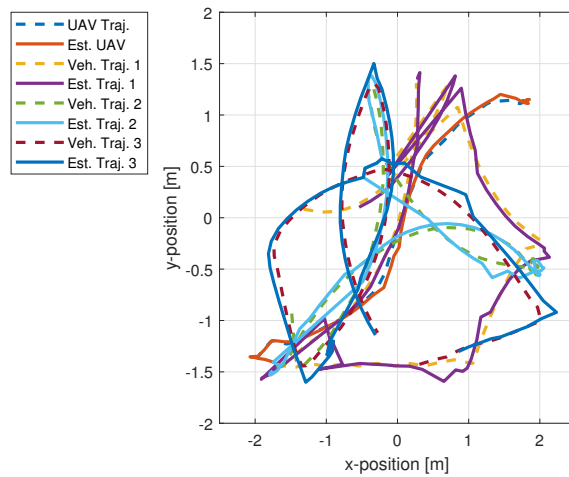
The tracking performance of both methods were compared by estimating their trajectories in occlusion situations as shown in Figure 7a,b. Both the LMIPDA-MC1 and LMIPDA-MC2 methods used the three-dimensional state propagation and process noise covariance matrices in Equation (6) to compute the motion of each vehicle, including the UAV. These matrices are same as expressed in Equations (27) and (28); however, the two-dimensional identity and zeros matrices must be converted in to three-dimensional matrices.

The UAV and autonomous vehicles trajectories are depicted by dashed colored lines, and their estimated trajectories are depicted by solid colored lines in Figure 7. We can see that the proposed LMIPDA-MC2 estimated the target motion more precisely and accurately without missing the target track. However, the LMIPDA-MC1 missed the target track at many intervals due to occlusion at different areas of surveillance especially in the region of $[-1.85, -0.82]^t$ m and $[-0.42, 1.4]^t$ m.



(a)

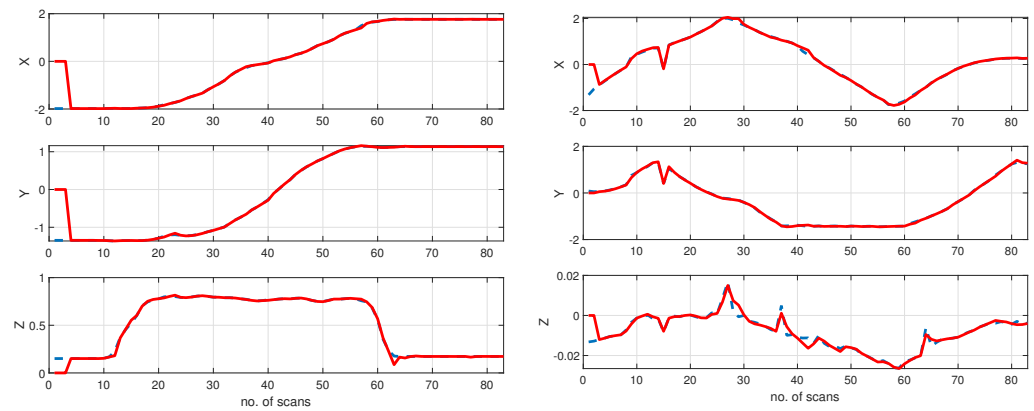
Figure 7. Cont.



(b)

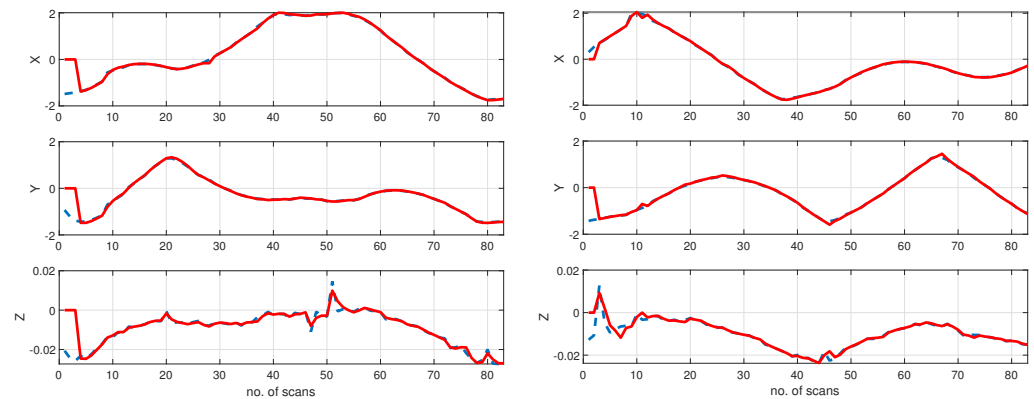
Figure 7. Tracking and estimation of each target trajectory: The original position of all autonomous vehicle (depicted by dashed colored lines) are reprinted from Expert Systems with Applications, 177, Myunggun Kim, Sufyan Ali Memon, et al., Dynamic based trajectory estimation and tracking in an uncertain environment, Page No. 8, Copyright (2021), with permission from Elsevier. (a) LMIPDA-MC2. (b) LMIPDA-MC1.

Figure 8 shows the position estimation of a UAV and autonomous vehicles in the x-, y- and z-axes using the proposed LMIPDA-MC2 method, whereas Figure 9 shows the position-estimation results of LMIPDA-MC1 in the three-dimensional coordinate system.



(a)

(b)



(c)

(d)

Figure 8. Position estimation of targets using LMIPDA–MC2. (a) UAV. (b) Autonomous vehicle 1. (c) Autonomous vehicle 2. (d) Autonomous vehicle 3.

It can be seen that the estimation accuracy in terms of position was significantly improved by using the MC2 model in the LMIPDA algorithm as show in Figure 8. The proposed method was also capable of tracking ground vehicles, which were moving randomly resulting in occlusions in the surveillance region. In contrast, the conventional LMIPDA (which is based on MC1) faced difficulties in detecting accurate position measurements of each target as depicted in Figure 9.

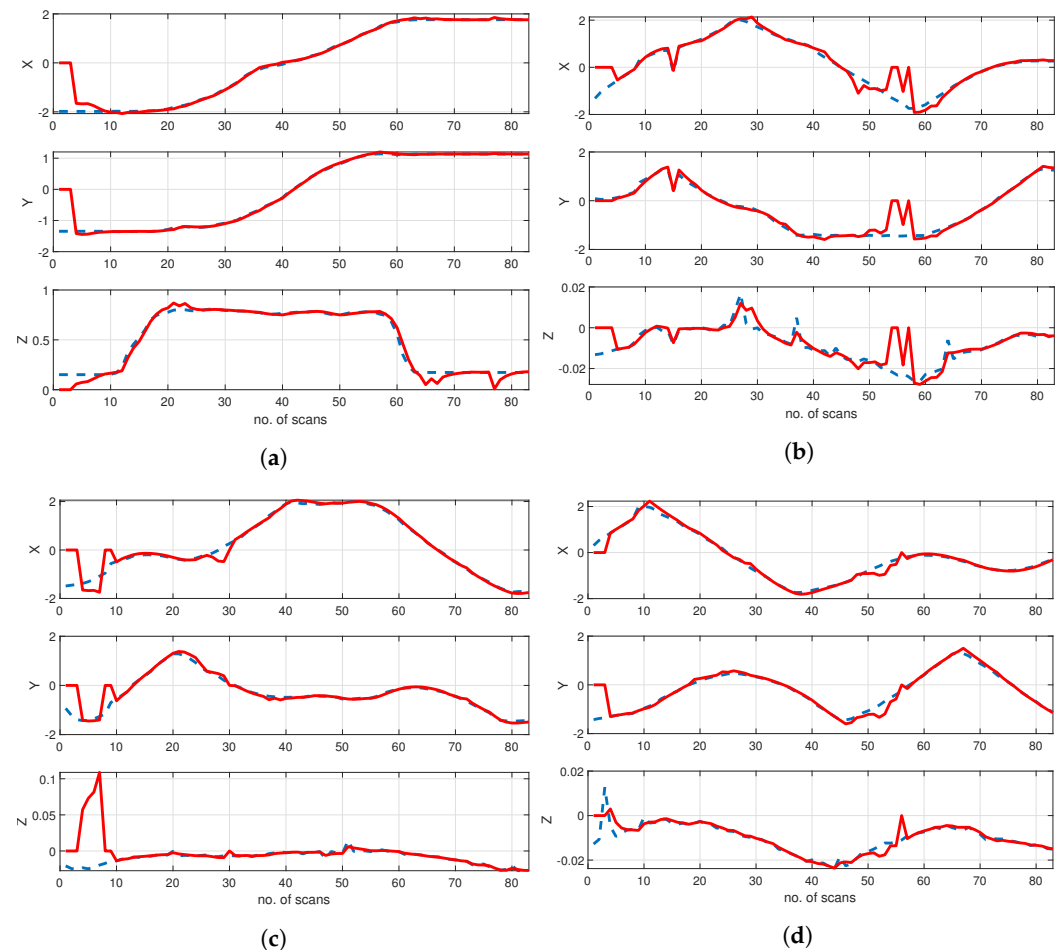


Figure 9. Position estimation of targets using LMIPDA–MC1. (a) UAV. (b) Autonomous vehicle 1. (c) Autonomous vehicle 2. (d) Autonomous vehicle 3.

Therefore, the experimental results show the redundancy of the MC1 model for the MTT system in an occlusion scenario. The RMSE of the estimated UAV trajectory based on the proposed LMIPDA-MC2 method was only 0.02, whereas that of the LMIPDA-MC1 method was equal to 0.04. Thus, the proposed LMIPDA-MC2 method improved the estimation accuracies, FTD and track retention as well as reduced the RMSE as compared to the existing reference methods.

6. Conclusions

We utilized the Markov-chain two (MC2) model in the proposed linear multi-target integrated probabilistic data association (LMIPDA-MC2) algorithm for tracking multi-targets at low-altitude airspace in an occluded and cluttered environment. The FTD performance of LMIPDA-MC2 improved the tracking of occluded targets and reduced the estimation errors when compared to other methods. In the experiment, the proposed method precisely tracked multiple moving vehicles at low altitude in occlusion, which shows the necessity of MC2 in multi-target-tracking systems. In addition, the track retention of the proposed method increased in each scan k .

The set of position measurements was generated using the motion capture camera in [32]. In this paper, we used only the position data to evaluate the LMIPDA-MC2 algorithm. The proposed idea is applicable for an intelligent multi-target-tracking system due to the capability of automatic track maintenance and propagation in occlusion. The probability of target existence (PTE) is a track-quality measure, which was used for confirming the true track and terminating the false track and, thus, evaluating the false-track discrimination (FTD).

Author Contributions: Conceptualization, H.S.; methodology, S.A.M. and U.K.; software, S.A.M.; validation, H.S., A.M.K. and M.S.; formal analysis, H.S., U.K. and M.S.; investigation, W.-G.K. and S.A.M.; resources, W.-G.K. and A.M.K.; data curation, W.-G.K. and U.K.; writing—original draft preparation, S.A.M.; writing—review and editing, U.K., A.M.K. and M.S.; supervision, H.S.; project administration, S.A.M. and H.S.; funding acquisition, S.A.M., H.S., W.-G.K., U.K. and M.S. All authors have read and agreed to the published version of the manuscript.

Funding: This research received no external funding.

Institutional Review Board Statement: Not applicable.

Informed Consent Statement: Not applicable.

Data Availability Statement: The research data presented in this study is available on request from the first author.

Acknowledgments: The experiments have been conducted in Ulsan National Institute of Science and Technology, Republic of Korea, with Memon, Sufyan Ali; Kim, Myunggun; and Shin, Minho under the supervision of Son, Hungsun. The position data of the multiple autonomous vehicles was generated using a motion capture camera, and the data were published in [32]. In this paper, we reused the original camera's position data for the evaluation of the proposed method.

Conflicts of Interest: The authors declare no conflict of interest.

References

1. Khaleghi, B.; Khamis, A.; Karray, F.O.; Razavi, S.N. Multisensor data fusion: A review of the state-of-the-art. *Inf. Fusion* **2013**, *14*, 28–44.
2. Garca, F.; Prioletti, A.; Cerri, P.; Broggi, A. PHD filter for vehicle tracking based on a monocular camera. *Expert Syst. Appl.* **2018**, *91*, 472–479.
3. Regragui, Y.; Moussa, N. A real-time path planning for reducing vehicles traveling time in cooperative-intelligent transportation systems. *Simul. Model. Pract. Theory* **2023**, *123*, 102710.
4. Furtado, J.S.; Lai, G.; Lacheray, H.; Desuoza-Coelho, J. *Advances in Motion Sensing and Control for Robotic Applications*; Janabi-Sharifi, F., Melek, M., Eds.; Chapter Comparative Analysis of OptiTrack Motion Capture Systems; Springer Nature: Cham, Switzerland, 2018; pp. 15–31.
5. Pattan, P.; Arjunagi, S. A human behavior analysis model to track object behavior in surveillance videos. *Meas. Sens.* **2022**, *24*, 100454.
6. Zhang, S.; Zheng, K.; Huaiyuan, S. Analysis of the Occlusion Interference Problem in Target Tracking. *Math. Probl. Eng.* **2022**, *2022*, 10.
7. Sebastian, D. Application of the Motion Capture System to Estimate the Accuracy of a Wheeled Mobile Robot Localization. *Energies* **2020**, *13*, 6437.
8. Challa, S.; Evans, R.; Morelande, M.; Mušicki, D. *Fundamentals of Object Tracking*; Cambridge University Press: New York, NY, USA, 2011.
9. Bar-Shalom, Y.; Daum, F.; Huang, J. The probabilistic data association filter. *IEEE Control Syst. Mag.* **2009**, *29*, 82–100.
10. Chen, X.; Li, Y.; Li, Y.; Yu, J.; Li, X. A Novel Probabilistic Data Association for Target Tracking in a Cluttered Environment. *Sensors* **2016**, *16*, 2180.
11. Mušicki, D.; Evans, R.; Stankovic, S. Integrated probabilistic data association. *IEEE Trans. Autom. Control* **1994**, *39*, 1237–1241.
12. Song, T.L.; Mušicki, D. Target tracking with target state dependent detection. *IEEE Trans. Signal Process.* **2011**, *59*, 1063–1074.
13. He, S.; Shin, H.-S.; Tsourdos, S. Multi-sensor multi-target tracking using domain knowledge and clustering. *IEEE Sens. J.* **2018**, *18*, 8074–8084. [[CrossRef](#)]
14. Ni, L.-Q.; Gao, S.-S.; Feng, P.-C.; Zhao, K. Rough Sets Probabilistic Data Association Algorithm and its Application in Multi-target Tracking. *Def. Technol.* **2013**, *9*, 208–2016. [[CrossRef](#)]
15. Sathyan, T.; Chin, T.; Arulampalam, S.; Suter, D. A Multiple Hypothesis Tracker for Multitarget Tracking with Multiple Simultaneous Measurements. *IEEE J. Sel. Top. Signal Process.* **2013**, *7*, 448–460. [[CrossRef](#)]

16. Mušicki, D.; Evans, R. JIPDA: Automatic target tracking avoiding track coalescence. *IEEE Trans. Aerosp. Electron. Syst.* **2015**, *51*, 962–974.
17. Asad, M.; Khan, S.; Mehmood, Z.; Shi, Y.; Memon, S.A.; Khan, U. A split target detection and tracking algorithm for ballistic missile tracking during the re-entry phase. *Def. Technol.* **2020**, *16*, 1142–1150.
18. Song, T.L.; Mušicki, D.; Yong, K. Multi-target tracking with state dependent detection. *IET Radar Sonar Navig.* **2015**, *9*, 10–18.
19. Lee, E.H.; Zhang, Q.; Song, T.L. Markov Chain Realization of Joint Integrated Probabilistic Data Association. *Sensors* **2017**, *17*, 2865.
20. Mušicki, D.; Scala, B.L. Multi-target tracking in clutter without measurement assignment. *IEEE Trans. Aerosp. Electron. Syst.* **2008**, *44*, 877–896. [[CrossRef](#)]
21. Mušicki, D.; Song, T. L.; Lee, H. Linear multitarget finite resolution tracking in clutter. *IEEE Trans. Aerosp. Electron. Syst.* **2014**, *50*, 1798–1812. [[CrossRef](#)]
22. Shin, M.; Son, H. Multiple Sensor Linear Multi-Target Integrated Probabilistic Data Association for Ultra-Wide Band Radar. *IEEE Access* **2020**, *8*, 227161–227171.
23. Huang, Y.; Song, T.L.; Kim, D. Linear Multitarget Integrated Probabilistic Data Association for Multiple Detection Target Tracking. *IET Radar Sonar Navig.* **2018**, *12*, 945–953. [[CrossRef](#)]
24. Mušicki, D.; Evans, R. Clutter map information for data association and track initialization. *IEEE Trans. Aerosp. Electron. Syst.* **2004**, *40*, 387–398. [[CrossRef](#)]
25. Wang, X.; Mušicki, D. Low elevation sea-surface target tracking using IPDA type filters. *IEEE Trans. Aerosp. Electron. Syst.* **2007**, *43*, 759–774. [[CrossRef](#)]
26. Song, T.L.; Mušicki, D.; Kim, Y. Tracking through Occlusions and Track Segmentation Reduction. *IEEE Trans. Aerosp. Electron. Syst.* **2013**, *49*, 623–631.
27. Kim, Y.; Song, T.L. A Study of Image Target Tracking Using ITS in an Occluding Environment. *J. Inst. Control Robot. Syst.* **2013**, *19*, 1457–1466. [[CrossRef](#)]
28. Song, T.L.; Musicki, D. Adaptive clutter measurement density estimation for improved target tracking. *IEEE Trans. Aerosp. Electron. Syst.* **2011**, *47*, 1457–1466. [[CrossRef](#)]
29. Grewal, M.S.; Andrews, A.P. *Kalman Filtering: Theory and Practice with MATLAB*; John Wiley and Sons: New York, NY, USA, 2014.
30. Jia, B.; Pham, K.; Blasch, E.; Shen, D.; Chen, G. Consensus-based auction algorithm for distributed sensor management in space object tracking. In Proceedings of the 2017 IEEE Aerospace Conference, Big Sky, MT, USA, 4–11 March 2017.
31. Bar-Shalom, Y.; Li, X.R.; Kirubarajan, T. *Estimation with Applications to Tracking and Navigation: Theory Algorithms and Software*; Wiley and Sons, Inc.: New York, NY, USA, 2004.
32. Kim, M.; Memon, S.A.; Shin, M.; Son, H. Dynamic based trajectory estimation and tracking in an uncertain environment. *Expert Syst. Appl.* **2021**, *177*, 114919.

Disclaimer/Publisher’s Note: The statements, opinions and data contained in all publications are solely those of the individual author(s) and contributor(s) and not of MDPI and/or the editor(s). MDPI and/or the editor(s) disclaim responsibility for any injury to people or property resulting from any ideas, methods, instructions or products referred to in the content.